ACS APPLIED MATERIALS & INTERFACES

Research Article

www.acsami.org

Modified Rheokinetic Technique to Enhance the Understanding of Microcapsule-Based Self-Healing Polymers

Timothy C. Mauldin,[†] Joshua Leonard,[‡] Kelly Earl,[‡] Jong Keun Lee,[§] and Michael R. Kessler*[,‡]

[†]Department of Chemistry, and [‡]Department of Materials Science and Engineering, Iowa State University, Ames, Iowa 50011, United States

[§]Department of Polymer Science and Engineering, Kumoh National Institute of Technology, Gumi, Gyungbuk 731-701, Republic of Korea

Supporting Information

ABSTRACT: A modified rheokinetic technique was developed to monitor the polymerization of healing monomers in a microcapsule-based, self-healing mimicking environment. Using this modified technique, monomers active toward ring-opening metathesis polymerization (ROMP) were either identified or disregarded as candidates for incorporation in self-healing polymers. The effect of initiator loading on the quality and speed of healing was also studied. It was observed that self-healing polymers have upper and lower temperature limits between which the healing mechanism performs at optimal levels. Also, a study of the quality of healing cracks of different thicknesses was performed, and it was discovered that above a critical crack thickness value, the quality of self-healing diminishes substantially; reasons for this phenomenon are discussed in detail.

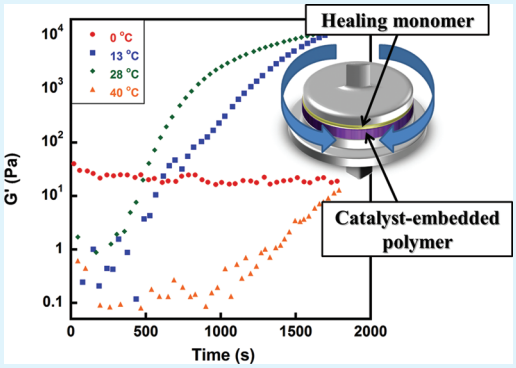

KEYWORDS: *self-healing, autonomic healing, crack-healing, rheokinetic, rheology, ROMP*

1. INTRODUCTION

In recent years, the development and refinement of self-healing polymers has garnered significant interest in both academic and industrial communities. Perhaps most indicative of the immense interest in this still relatively young field of research is the large number of review articles that have appeared in the literature, the majority within the last half-decade.[1−18] Although several fundamentally different healing mechanisms have been developed, each targeted toward their own commercial niche, self-healing polymers containing microencapsulated healing components[19−23] have received a significant amount of the attention. In this healing mechanism, microcapsules containing liquid ring-opening metathesis-based monomer are embedded within a polymer matrix, along with ruthenium olefin metathesis catalyst particles. When damage occurs, cracks propagate through the polymer matrix, rupturing the embedded microcapsules. The encapsulated liquid monomer is then able to flow into the damage region and contact the catalyst particles, polymerize, and join the crack surfaces together.

Although this mechanism of healing may initially seem straightforward, significant optimization of the healing components is required before these materials can be considered for commercial use. For example, microcapsules and catalyst must be compatible with standard polymer processing techniques (e.g., the high pressures of some melt-processing techniques, high-temperature curing cycles, etc.). The physical properties of the liquid healing monomer must allow for easy flow into the damage region (i.e., low viscosity), to minimize loss caused by volatilization and/or diffusion into the polymer matrix, and for good wetting of the crack surface. Dissolution of the catalyst in the liquid monomer, as well as the subsequent polymerization kinetics, must also be tailored accordingly. And finally, the resulting polymer must have sufficient adhesive and mechanical properties to mitigate further damage. With this daunting set of requirements in mind, much of our previous work has focused on the evaluation of healing monomers through thermal analysis and mechanical testing.[24−31] These techniques are designed to be versatile, relatively quick and easy to use, and they often yield the copious amounts of quantitative data necessary to adequately design and screen different healing components. However, because of several complexities of the self-healing mechanism, these ex-situ analytical techniques are only a complement to, and not a substitute for, the evaluation of healing formulations through actual fabrication and testing of self-healing materials. Direct evaluation of self-healing materials is most often done by fabricating fracture specimens containing embedded healing components. Upon initially failing the specimens under mechanical load, the fracture halves are brought into contact and allowed to heal, after which point the resulting healed specimens can be subsequently retested. Tapered double-cantilever beam geometry fracture specimens were initially used for this purpose,[32−34] as this geometry yields

Received: January 23, 2012
Accepted: March 1, 2012
Published: March 1, 2012

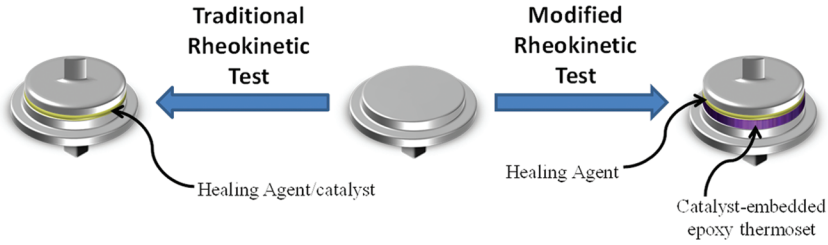

Figure 1. Schematic representation of a traditional rheokinetic experiment (left arrow) and the modified rheokinetic experiments with a polymer-coated bottom plate (right arrow).

some fracture properties that are independent of crack length, which otherwise may vary from a pristine sample to its healed sample.[35] Although these techniques are more laborious and use much more material than the ex-situ analyses mentioned above, they are crucial in that they provide not only an actual demonstration of healing, but also some quantitative descriptions of that healing by virtue of comparison of mechanical properties of virgin vs healed specimens.

The goal of this work is to develop an analytical technique that collapses the dichotomy between the ex situ and direct evaluation methods of self-healing polymers. In other words, we have developed a novel technique that simulates the self-healing mechanism, yet is quick, easy to perform, requires very little material, and yields large amounts of quantitative data. To do this, we modified a traditional parallel plate rheological technique in such a way that mimics a self-healing polymer, as shown in Figure 1. The center image represents a bottom rheometer parallel plate with a material layer placed on top. By adding a top rheometer plate and applying a shear force, rheological properties of the examined material under various stimuli (e.g., time, temperature, shear rate, etc.) can be measured. For example, the left arrow in Figure 1 shows a traditional rheokinetic setup in which the developing rheological properties of a polymerizing monomer/catalyst solution can be determined. In our modified rheokinetic technique, however, we use the rheometer bottom plate as a scaffold to build a pseudo self-healing polymer. This is done by first coating the bottom plate with a catalyst-embedded polymer, and then polishing the surface of the modified plate to reveal catalyst particles. Then, upon injecting liquid monomer on the surface of the modified plate, catalyst dissolution and polymerization must occur concurrently in a confined environment (Figure 1, right arrow), roughly in the same manner as they occur during the self-healing mechanism. Preliminary efforts have already shown the successful utilization of this technique to rapidly screen different healing monomers, catalysts, and polymer matrices suitable for self-healing materials.[36,37] Here, we further expand this modified rheokinetic technique to identify its limitations as well as probe the effects of self-healing material design parameters (e.g., monomer identity, catalyst identity, amount of healing components used, etc.) on the self-healing mechanism. Also, successful implementation of this technique has led to the discovery of unexpected interface phenomena and, to the best of our knowledge, previously unknown limitations to self-healing related both to temperature and to the thickness of the damage region that requires healing.

2. RESULTS AND DISCUSSION

Microcapsule-based self-healing polymers have utilized a number of different healing chemistries, such as epoxide ring-opening,[38−45] "click" chemistry,[46−48] siloxane polycondensation,[49,50] radical polymerization,[51−53] and ring-opening metathesis polymerization (ROMP).[54−63] Ring-opening metathesis polymerization of dicyclopentadiene (DCPD) with Grubbs' olefin metathesis catalyst[64−66] is notable as one of the first polymerization mechanisms demonstrated to work well in self-healing polymers.[67] For this reason, ROMP with the first generation Grubbs' catalyst was chosen as a healing chemistry for this work, but we envision that the rheokinetic technique presented here is versatile enough to be applicable toward evaluating other types of healing chemistries and other healing formulations, such as catalyst protection techniques.[68]

Our original motivation for developing this modified rheokinetic technique was to rapidly screen different healing monomers in order to identify ideal candidates that offer a good balance of catalyst dissolution kinetics and polymerization kinetics. To this end, evolution of dynamic mechanical properties in the modified rheokinetic technique was monitored for several ROMP-active monomers. For the sake of concision, only a small subset of these monomers with a wide range of reactivities are presented here; their chemical structures and name abbreviations are shown in Figure 2. Specifically, Figure 3

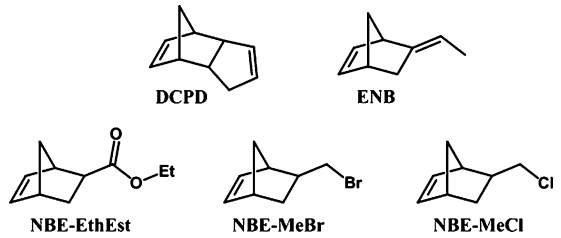

Figure 2. Chemical structures and abbreviations of several ROMP-active monomers.

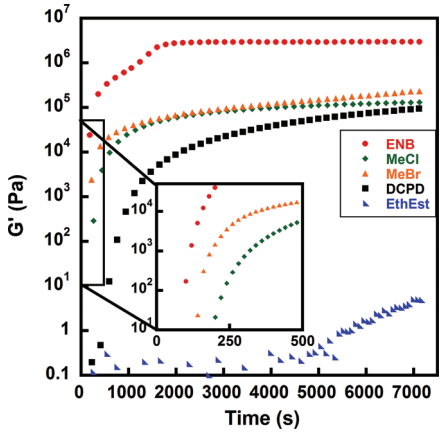

Figure 3. Evolution of shear storage modulus (G') of several ROMP-active healing monomer candidates.

shows the evolution of G' with respect to time during the polymerization reaction of each of these monomers. Monomers ENB, NBE-MeBr, and NBE-MeCl show superior rheokinetics, with gelation times of 170 ± 10, 181 ± 15, and 281 ± 18 s, respectively. All three of these monomers gel considerably faster than DCPD (gelation time of 682 ± 45 s), which is notable because DCPD is sometimes considered as a "benchmark" healing monomer for its superior healing precedent in previous work.[67] ENB seems particularly attractive as a healing monomer candidate, as it attains its maximum G′ value in roughly 30 min, almost an order of magnitude faster than all other monomers studied here. NBE-EthEst showed the slowest rheokinetics of the five monomers studied, with any measurable growth of storage modulus occurring only after approximately 90 min and no gelation (i.e., no G', G'' crossover) over the course of this experiment. This is consistent with previous reports of low ROMP reactivity of norbornenyl derivatives with oxygen containing functional groups.[69,70] Although these data imply that NBE-EthEst would likely not be a successful healing monomer, this demonstrates that our modified rheokinetic technique is not only useful to select promising healing monomer candidates, but also useful to quickly discard less favorable candidates.

One important consideration in developing microcapsule-based self-healing materials is the amount of healing additives that should be added to the overall polymer matrix. On the one hand, lower loadings of healing additives are preferred in order to reduce overall material cost and inhibit reduction in the virgin polymer's properties. On the other hand, loadings should not be so low that the quality and speed of healing is negatively affected. Although traditional techniques to determine optimal loadings of healing additives in self-healing polymers would likely include the potentially long and tedious tasks of fabricating and testing fracture specimens with various combinations and loadings of healing components, the present modified rheokinetic technique is ideally suited to quickly and efficiently answer these types of questions. For example, Figure 4 shows the effect of catalyst

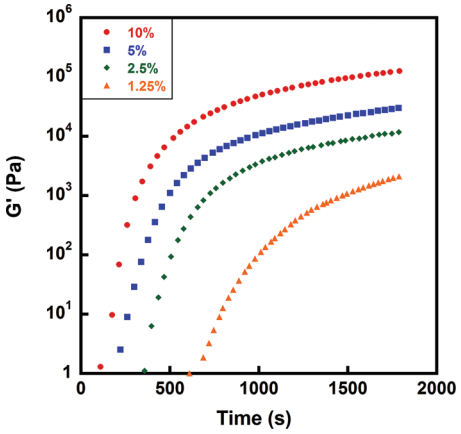

Figure 4. Evolution of G' during polymerization of DCPD with different loadings of Grubbs' catalyst in the modified rheometer plate coating. Percentage loadings of catalyst are wt/wt% with respect to the epoxy coating.

particle loading in the modified rheometer plate setup on the evolution of DCPD's storage modulus. As expected, increasing loadings of the catalyst clearly accelerates the polymerization reaction, and higher loadings of catalyst yield polymers with a higher overall G' at any given time.

Considering the fact that self-healing polymers could be utilized for outdoor applications, in which temperatures significantly fluctuate based on the time of day, season, and global location, it is of interest to obtain a detailed understanding of how the quality and kinetics of self-healing changes with temperature. Figure 5 shows the change in G' of DCPD over a

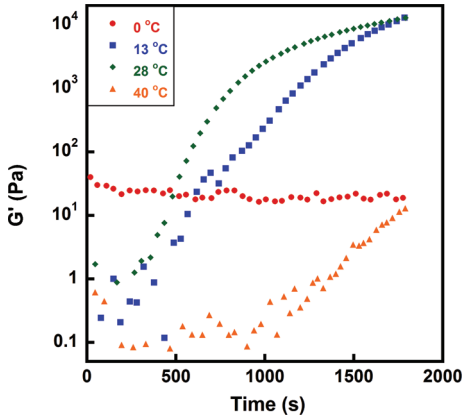

Figure 5. Evolution of G' during the polymerization of DCPD on modified rheometer plates at different isothermal temperatures.

range of different isothermal temperatures, chosen to simulate exposure temperatures experienced in outdoor environments. At 0 °C, there is no observable growth of G' throughout the course of this experiment. This is likely because 0 °C is below the melting temperature of DCPD (8–9 °C), and thus DCPD remains a solid at this temperature. Presumably, solid DCPD does not have the ability to dissolve catalyst from the modified rheometer plate, and therefore no reaction is expected to take place. Upon increasing the temperature above DCPD's melting temperature to 13 °C, growth in G′ is observed, although with a relatively long gelation time of 1027 ± 48 s. Increasing the temperature to 28 °C further accelerates the polymerization and results in a gelation time of 364 ± 41 s. However, increasing the temperature to 40 °C initially appears to slow the polymerization, contrary to what may be expected at elevated temperatures. Visual observation of the bottom rheometer plate after immediate removal from the instrument revealed a layer of polymer film directly covering the modified bottom plate, on top of which was a layer of liquid monomer DCPD (Figure 6). It is believed that

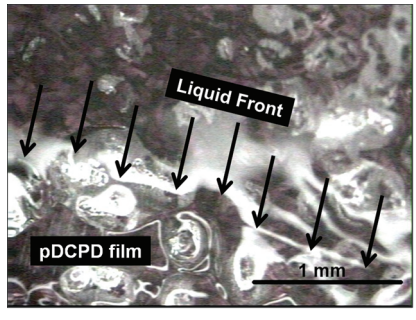

Figure 6. Optical microscope image of a rheometer bottom plate showing a layer of liquid DCPD above a layer of polymerized DCPD. Image was taken looking downward at the top of a modified rheometer bottom plate immediately after a 30 min rheokinetic test at an isothermal temperature of 40 °C.

the rheological inference that the kinetics decreases at higher temperatures is not correct, but rather that the polymerization

reaction is in fact so rapid that it quickly gels around the catalyst particles, quenching further dissolution of catalyst and slowing diffusion of catalyst into the upper layer of liquid monomer. The fact that samples at elevated temperatures exhibit obvious property gradients through the sample thickness complicates any rheological interpretation of these data, but these results demonstrate that the self-healing mechanism has a heightened sensitivity to moderately high temperatures.

By visual inspection, Figure 6 shows that the stiffest layers of polymer exist in close proximity to the bottom rheometer plate, which serves as a catalyst source, and stiffness decreases with increasing distance from the modified plate surface. The likely reason for the direction of this property gradient is that catalyst dissolved from the modified rheometer plate is effective first in the bottom layers of the monomer and then must diffuse toward the top layers of monomer. This led to the question of whether healing is significantly affected by the thickness of the liquid monomer sample, i.e., whether thicker samples may require more time to diffuse catalyst through to the top layers of monomer. With respect to self-healing polymers, this question has implications regarding the capability of healing cracks of different thickness. To test these hypotheses, rheological experiments were performed with varying the gap sizes (i.e., the distance from the top rheometer plate surface to the modified bottom plate surface), which required varying amounts of monomer to fill the different sized gaps. Gap size was varied by adjusting the volume of monomer delivered to the gap region. Delivering 0.1, 0.3, and 0.5 mL of DCPD to the gap region yielded average starting gap sizes (i.e., gap sizes immediately after monomer injection, prior to any gap shrinkage upon polymerization) of 180 ± 9, 534 ± 41, and 839 ± 58 μm, respectively. Figure 7 shows how gelation time, vitrification time, and G'_{final} change with changing gap size. Also, as a control test, Figure 7 shows the dependence of these three variables on gap size in unmodified rheology experiments, in which catalyst and monomer were premixed (2 mg/mL catalyst/monomer) and injected on an unmodified bottom rheometer plate.

The values measured in the modified and unmodified rheokinetic tests cannot be directly compared, because the amount of catalyst dissolved in monomer during the modified rheokinetic tests is unknown, but interpretations can be made based on the sensitivity of rheological property development to gap size. As seen in Figure 7a,b, gelation time and vitrification time change considerably with different gap sizes when using the modified rheometer plates. Considering the fact that these times show almost no dependence on gap size when using unmodified plates, it is very likely that this effect is related to through-thickness property gradients resulting from slow diffusion of catalyst from the modified plate through to the upper layers of monomer. This was visually confirmed by removing the parallel plates from the instrument after gelation, but prior to vitrification; the DCPD samples on the modified bottom parallel plates were very tacky on the surface, while the subsurface layers just above the modified plate surface consisted of stiffer polymer. However, Figure 7c indicates that final shear storage modulus, G'_{final}, seems to be mostly insensitive to gap size, independently of whether modified or unmodified parallel plates were used. This implies that a sufficient amount of catalyst will eventually permeate throughout the entire sample thickness, which is reasonable considering the fact that diffusion is a kinetic event only and should not affect the thermodynamically dominated steady-state storage modulus.

Especially surprising is how sensitive gelation and vitrification are to gap size, specifically for gap sizes >200 μm. It does appear that for gap sizes <200 μm, however, there is minimal deviation between data obtained from modified and unmodified plates. One plausible explanation for this is that catalyst can diffuse relatively quickly through the liquid monomer until a significant increase in monomer viscosity occurs because of the onset of polymerization, at which time catalyst diffusion is retarded. When interpreting these data with respect to the self-healing mechanism, it must be taken into consideration that only the bottom rheometer parallel plate (i.e., not the top parallel plate) is coated with a catalyst/epoxy layer, while in a self-healing polymer both crack surfaces would contain embedded catalyst particles that can contribute to the chemical reaction. Therefore, the behavior observed in the rheometer gap is assumed to be roughly equivalent to the behavior in a self-healing polymer with half the crack thickness. If this assumption is correct, it would appear that crack thicknesses <400 μm would be mostly unaffected by this catalyst diffusion phenomenon, while the healing kinetics of cracks with thicknesses >400 μm could be significantly affected by crack size. While a crack thickness value of ~400 μm can hardly be considered a universal critical value (this value would change for different monomers, catalysts, temperatures, etc.), it is important because it is on the approximate size scale expected for larger delamination thicknesses in fiber-reinforced composite materials and moderate-sized macrocracks. Although Rule and co-workers also noted advantages of healing smaller crack

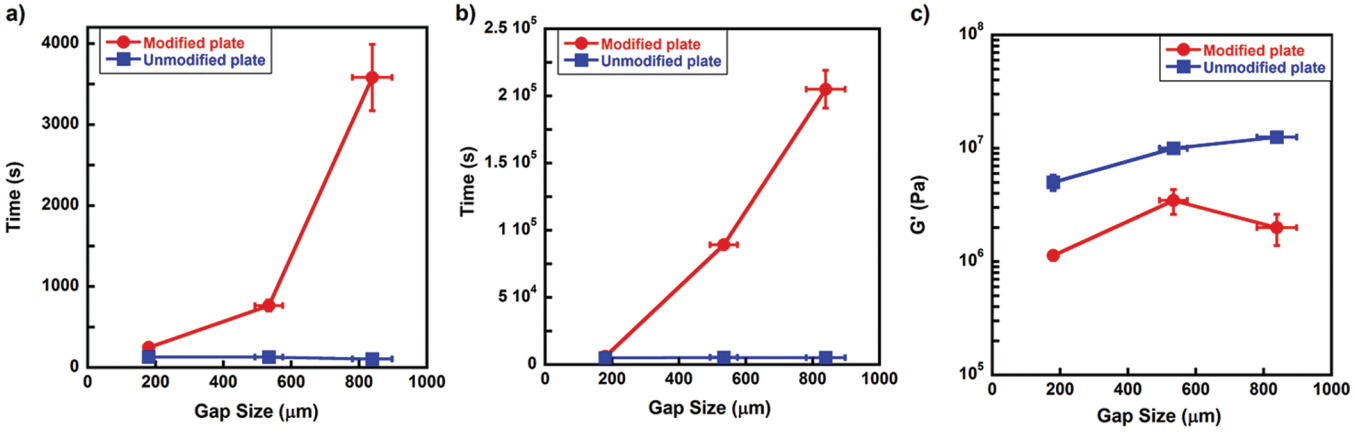

Figure 7. Dependence of (a) gel time, (b) vitrification time, and (c) G'_{final} on gap size during modified and unmodified rheological experiments.

sizes,[71] their conclusions were based on issues related to ensuring a sufficient supply of healing monomer to damage volumes; to the best of our knowledge, this work is the first observation of catalyst diffusion-based property gradients in healing monomers.

3. CONCLUSIONS

Rheometer bottom parallel plates were modified with a catalyst-embedded epoxy coating in order to mimic a crack surface of a fractured microcapsule-based, self-healing polymer. Using these modified rheometer plates, rheokinetic analyses were performed on healing monomers in a pseudo self-healing environment. It was demonstrated that this technique could be used to quickly and efficiently develop a tailored self-healing polymer by rapidly screening the effect of various design parameters (e.g., monomer and catalyst identity, catalyst loading, etc.) on the quality and speed of healing. Additionally, the simplicity and versatility of this technique, coupled with its substantial quantitative outputs, allowed for the identification of two previously unknown limitations to the self-healing mechanism—upper/lower temperature limits and large crack thicknesses—that are ultimately linked to transfer of catalyst through the monomer/crack surface interface.

4. EXPERIMENTAL SECTION

Dicyclopentadiene (DCPD, endo-isomer), benzylidene-bis-(tricyclohexylphosphine) dichlororuthenium (first generation Grubbs' Catalyst), and 5-ethylidene-2-norbornene (ENB) were all purchased from Aldrich and used as received. EPON 828 Epoxy Resin, and EPIKURE 3223 Curing Agent (diethylenetriamine) were bought from Miller-Stephenson and also used as received. Literature methods were used to prepare 5-chloromethyl-2-norbornene,[72] 5-bromomethyl-2-norbornene,[73] and ethyl 5-norbornene-2-carboxylate.[74] Rheological tests were performed using an AR2000ex stress-controlled rheometer (TA Instruments) with parallel plate geometry. Aluminum parallel plates with a 25 mm diameter were purchased from TA Instruments.

Rheometer Bottom Plate Modification. EPON 828 epoxy resin was vigorously hand-stirred with 14 pph diethylenetriamine and degassed at ambient temperature under high vacuum for 15 min. In most cases, first-generation Grubbs' catalyst was gently hand-stirred into the solution until the catalyst particles were well dispersed, as verified by visual inspection. Unless otherwise noted, 2.5 wt/wt% catalyst particles were added to the epoxy resin. The suspension was poured into custom-designed, open silicone rubber molds with center-bored cylinders and one vent hole, and rheometer bottom parallel plates were inverted and fixed into the cylinder so that the drip channel rested snug on the top of the mold (see the Supporting Information for custom-designed mold schematics). Molds were placed in a 65 °C preheated oven for 1 h, resulting in an epoxy-based disk coating bonded to the rheometer plate surface with precise dimensions of 25 mm diameter and 2 mm thickness. Catalyst particles showed excellent dispersion in the final samples (shown in the Supporting Information). Catalyst was revealed on the surface of the plates by hand-polishing the coating immediately, first with 600 grit sandpaper followed by 2000 grit sandpaper. Polishing was done immediately prior to each rheology experiment in order to ensure that catalyst's exposure to air occurred only for a matter of minutes, which negligibly decomposes the catalyst.[75,76]

Rheology Procedure. Rheological experiments were conducted as follows (unless otherwise noted in the text): Top and bottom rheometer plates were fixed to the instrument, and 0.25 mL of 5 vol/vol% ENB in DCPD mixture was injected on the bottom plate with a 1-ml syringe. The 5% ENB was used as a reactive diluent to lower DCPD's melting point to 8−9 °C (measured by differential scanning calorimetry: TA Instruments Q20 model at a heating rate of 5 K/min over a range of 0−50 °C), and the mixture will be referred to simply as DCPD. In some cases, a premixed catalyst and monomer solution was added to the unmodified bottom plates. In either case, the time at which the monomer first contacted the catalyst particles until data collection began was recorded with a stopwatch, and that time was artificially added to the start of each test (e.g., if the monomer was in contact with the catalyst for 10 s prior to the start of data collection, then the data point at which t = 0 s was shifted to t = 10 s, and all other data points were shifted accordingly). Oscillatory shear experiments were used to monitor changes in shear dynamic mechanical properties (G' = shear storage modulus, G'' = shear loss modulus, and tan δ = G''/G'). Initially, experiments were run in a strain-controlled setting at a strain of 5% and a frequency of 1 Hz. A strain of 5% was chosen as an optimal value that provides enough torque to collect data on low-viscosity liquids with an acceptable level of noise, but is also a small enough shear rate so as not to artificially aid catalyst dissolution in the monomer. Once the modulus of the material developed requires a shear stress of 1000 Pa to attain the 5% strain, the experiment was programmed to switch to a stress-controlled setting with a constant shear stress of 1000 Pa and a frequency of 1 Hz. This change in testing mode was implemented to accommodate the high sample moduli reached at the end of each experiment, which in a strain-controlled setting would otherwise require shear stresses outside of instrument limits to attain a shear strain of 5%. Also, unless noted otherwise, all tests were performed at 23 °C. Gelation time is defined here as the time at which the polymer loses its ability to flow, signified by the G' and G'' curves crossover; and vitrification time is defined as the time after the gelation time at which tan δ is at a maximum. Figure 8 graphically depicts how each of these variables is chosen in a representative rheokinetic plot. All reported values of gelation time, vitrification time, and G'_{final} are averages over three experiments.

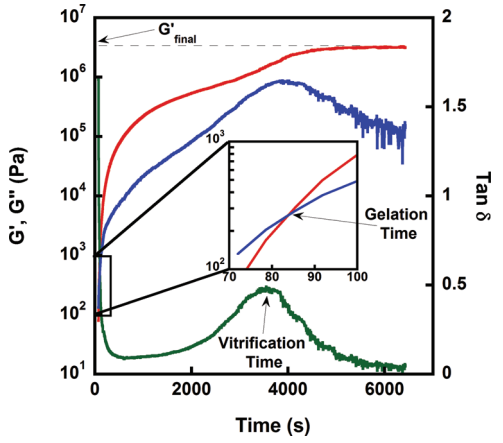

Figure 8. Representative rheokinetic plot showing the evolution of G' (red), G'' (blue), and tan δ (green). Gelation time was taken as the crossover between the G' and G'' plots, vitrification time was defined as the maximum of the tan δ curve (after gelation), and G'_{final} is modulus at which G' reaches a steady-state.

■ ASSOCIATED CONTENT

Ⓢ Supporting Information

Mold schematics and additional optical micrographs. This material is available free of charge via the Internet at http://pubs.acs.org/.

■ AUTHOR INFORMATION

Corresponding Author

*E-mail: mkessler@iastate.edu.

Notes

The authors declare no competing financial interest.

■ ACKNOWLEDGMENTS

This work was supported by The American Chemical Society Petroleum Research Fund (ACS PRF 47700-AC7) and the

National Science Foundation (Award 0954314). The authors gratefully acknowledge Dr. Xing Liu and Dr. Xia Sheng for rheometer assistance and helpful discussions.

REFERENCES

(1) Williams, K. A.; Dreyer, D. R.; Bielawski, C. W. *MRS Bull.* **2008**, *33*, 759−765.
(2) Trask, R. S.; Williams, H. R.; Bond, I. P. *Bioinsp. Biomim.* **2007**, *2*, 1−9.
(3) Mauldin, T. C.; Kessler, M. R. *Int. Mater. Rev.* **2010**, *55*, 317−346.
(4) Wu, D. Y.; Meure, S.; Solomon, D. *Prog. Polym. Sci.* **2008**, *33*, 479−522.
(5) van der Zwaag, S.; van Dijk, N. H.; Jonkers, H. M.; Mookhoek, S. D.; Sloof, W. G. *Philos. Trans. R. Soc. London, Ser. A* **2009**, *367*, 1689−1704.
(6) Kessler, M. R. *Proc. Inst. Mech. Eng., Part G* **2007**, *221*, 479−495.
(7) Murphy, E. B.; Wudl, F. *Prog. Polym. Sci.* **2010**, *35*, 223−251.
(8) Yuan, Y. C.; Yin, T.; Rong, M. Z.; Zhang, M. Q. *Express Polym. Lett.* **2008**, *2*, 238−250.
(9) White, S. R.; Caruso, M. M.; Moore, J. S. *MRS Bull.* **2008**, *33*, 766−769.
(10) Wool, R. P. *Soft Matter* **2008**, *4*, 400−418.
(11) Brochu, A. B. W.; Craig, S. L.; Reichert, W. M. *J. Biomed. Mater. Res. Part A* **2011**, *96A*, 492−506.
(12) Wang, H. P.; Rong, M. Z.; Zhang, M. Q. *Prog. Chem.* **2010**, *22*, 2397−2407.
(13) Syrett, J. A.; Becer, C. R.; Haddleton, D. M. *Polym. Chem.* **2010**, *1*, 978−987.
(14) Samadzadeh, M.; Boura, S. H.; Peikari, M.; Kasiriha, S. M.; Ashrafi, A. *Prog. Org. Coat.* **2010**, *68*, 159−164.
(15) Blaiszik, B. J.; Kramer, S. L. B.; Olugebefola, S. C.; Moore, J. S.; Sottos, N. R.; White, S. R. *Annu. Rev. Mater. Res.* **2010**, *40*, 179−211.
(16) Bergman, S. D.; Wudl, F. *J. Mater. Chem.* **2008**, *18*, 41−62.
(17) Urban, M. W. *Prog. Polym. Sci.* **2009**, *34*, 679−687.
(18) Burattini, S.; Greenland, B. W.; Chappell, D.; Colquhoun, H. M.; Hayes, W. *Chem. Soc. Rev.* **2010**, *39*, 1973−1985.
(19) Brown, E. N.; Kessler, M. R.; Sottos, N. R.; White, S. R. *J. Microencapsulation* **2003**, *20*, 719−730.
(20) Liu, X.; Sheng, X; Lee, J. K.; Kessler, M. R. *Macromol. Mater. Eng.* **2009**, *294*, 389−395.
(21) Brown, E. N.; White, S. R.; Sottos, N. R. *J. Mater. Sci.* **2004**, *39*, 1703−1710.
(22) Kessler, M. R.; Sottos, N. R.; White, S. R. *Composites, Part A* **2003**, *34*, 743−753.
(23) Kessler, M. R.; White, S. R. *Composites, Part A* **2001**, *32*, 683−699.
(24) Liu, X.; Sheng, X.; Lee, J. K.; Kessler, M. R. *J. Therm. Anal. Calorim.* **2007**, *89*, 453−457.
(25) Larin, G. E.; Bernklau, N.; Kessler, M. R.; DiCesare, J. C. *Polym. Eng. Sci.* **2006**, *46*, 1804−1811.
(26) Liu, X.; Lee, J. K.; Yoon, S. H.; Kessler, M. R. *J. Appl. Polym. Sci.* **2006**, *101*, 1266−1272.
(27) Sheng, X.; Kessler, M. R.; Lee, J. K. *J. Therm. Anal. Calorim.* **2007**, *89*, 459−464.
(28) Sheng, X.; Lee, J. K.; Kessler, M. R. *Polymer* **2009**, *50*, 1264−1269.
(29) Jeong, W.; Kessler, M. R. *Chem. Mater.* **2008**, *20*, 7060−7068.
(30) Jeong, W.; Kessler, M. R. *Carbon* **2009**, *47*, 2406−2412.
(31) Mauldin, T. C.; Kessler, M. R. *J. Mater. Chem.* **2010**, *20*, 4198−4206.
(32) Brown, E. N.; Sottos, N. R.; White, S. R. *Exp. Mech.* **2002**, *42*, 372−379.
(33) Brown, E. N.; White, S. R.; Sottos, N. R. *Compos. Sci. Technol.* **2005**, *65*, 2466−2473.
(34) Brown, E. N.; White, S. R.; Sottos, N. R. *Compos. Sci. Technol.* **2005**, *65*, 2474−2480.
(35) Brown, E. N. *J. Strain. Anal. Eng. Des.* **2011**, *46*, 167−186.
(36) Lee, J. K.; Liu, X.; Yoon, S. H.; Kessler, M. R. *J. Polym. Sci., Part B: Polym. Phys.* **2007**, *45*, 1771−1780.
(37) Liu, X.; Sheng, X.; Kessler, M. R.; Lee, J. K. *Compos. Sci. Technol.* **2009**, *69*, 2101−2107.
(38) Rong, M. Z.; Zhang, M. Q.; Zhang, W. *Adv. Compos. Lett.* **2007**, *16*, 167−172.
(39) Yin, T.; Rong, M. Z.; Zhang, M. Q.; Yang, G. C. *Compos. Sci. Technol.* **2007**, *67*, 201−212.
(40) Yin, T.; Rong, M. Z.; Zhang, M. Q.; Zhao, J. Q. *Smart Mater. Struct.* **2009**, *18*, 1−7.
(41) Yin, T.; Rong, M. Z.; Zhang, M. Q. *Adv. Mater. Res.* **2008**, *47*−*50*, 282−285.
(42) Yin, T.; Zhou, L.; Rong, M. Z.; Zhang, M. Q. *Smart Mater. Struct.* **2008**, *17*, 1−8.
(43) Yin, T.; Rong, M. Z.; Wu, J.; Chen, H.; Zhang, M. Q. *Composites, Part A* **2008**, *39*, 1479−1487.
(44) Yuan, Y. C.; Rong, M. Z.; Zhang, M. Q.; Chen, J.; Yang, G. C.; Li, X. M. *Macromolecules* **2008**, *41*, 5197−5202.
(45) Xiao, D. Z.; Yuan, Y. C.; Rong, M. Z.; Zhang, M. Q. *Polymer* **2009**, *50*, 2967−2975.
(46) Sheng, X.; Mauldin, T. C.; Kessler, M. R. *J. Polym. Sci., Part A: Polym. Chem.* **2010**, *48*, 4093−4102.
(47) Gragert, M.; Schunack, M.; Binder, W. H. *Macromol. Rapid Commun.* **2011**, *32*, 2011.
(48) Schunack, M.; Gragert, M.; Dohler, D.; Michael, P.; Binder, W. H. *Macromol. Chem. Phys.* **2012**, *213*, 205−214.
(49) Keller, M. W.; White, S. R.; Sottos, N. R. *Adv. Funct. Mater.* **2007**, *17*, 2399−2404.
(50) Keller, M. W.; White, S. R.; Sottos, N. R. *Polymer* **2008**, *49*, 3136−3145.
(51) Yao, L.; Yuan, Y. C.; Rong, M. Z.; Zhang, M. Q. *Polymer* **2011**, *52*, 3137−3145.
(52) Yao, L.; Rong, M. Z.; Zhang, M. Q.; Yuan, Y. C. *J. Mater. Chem.* **2011**, *21*, 9060−9065.
(53) Wang, H. P.; Yuan, Y. C.; Rong, M. Z.; Zhang, M. Q. *Macromolecules* **2010**, *43*, 595−598.
(54) Kessler, M. R.; White, S. R. *J. Polym. Sci., Part A: Polym. Chem.* **2002**, *40*, 2373−2383.
(55) Jones, A. S.; Rule, J. D.; Moore, J. S.; Sottos, N. R.; White, S. R. *J. R. Soc. Interface* **2007**, *4*, 395−403.
(56) Wilson, G. O.; Moore, J. S.; White, S. R.; Sottos, N. R.; Andersson, H. M. *Adv. Funct. Mater.* **2008**, *18*, 44−52.
(57) Rule, J. D.; Moore, J. S. *Macromolecules* **2002**, *35*, 7878−7882.
(58) Mauldin, T. C.; Rule, J. D.; Sottos, N. R.; White, S. R.; Moore, J. S. *J. R. Soc. Interface* **2007**, *4*, 389−393.
(59) Lee, J. K.; Hong, S. J.; Liu, X.; Yoon, S. H. *Macromol. Res.* **2004**, *12*, 478−483.
(60) Jones, A. S.; Rule, J. D.; Moore, J. S.; White, S. R.; Sottos, N. R. *Chem. Mater.* **2006**, *18*, 1312−1317.
(61) Wilson, G. O.; Caruso, M. M.; Reimer, N. T.; White, S. R.; Sottos, N. R.; Moore, J. S. *Chem. Mater.* **2008**, *20*, 3288−3297.
(62) Rule, J. D.; Brown, E. N.; Sottos, N. R.; White, S. R.; Moore, J. S. *Adv. Mater.* **2005**, *17*, 205−208.
(63) Kamphaus, J. M.; Rule, J. D.; Moore, J. S.; Sottos, N. R.; White, S. R. *J. R. Soc. Interface* **2008**, *5*, 95−103.
(64) Grubbs, R. H. *Angew. Chem., Int. Ed.* **2006**, *45*, 3760−3765.
(65) Nguyen, S. T.; Grubbs, R. H. *J. Am. Chem. Soc.* **1993**, *115*, 9858−9859.
(66) Dias, E. L.; Nguyen, S. T.; Grubbs, R. H. *J. Am. Chem. Soc.* **1997**, *119*, 3887−3897.
(67) White, S. R.; Sottos, N. R.; Geubelle, P. H.; Moore, J. S.; Kessler, M. R.; Sriram, S. R.; Brown, E. N.; Viswanathan, S. *Nature* **2001**, *409*, 794−797.
(68) Rule, J. D.; Brown, E. N.; Sottos, N. R.; White, S. R.; Moore, J. S. *Adv. Mater.* **2005**, *17*, 205−208.
(69) Haigh, D. M.; Kenwright, A. M.; Khosravi, E. *Tetrahedron* **2004**, *60*, 7217−7224.
(70) Czelusniak, I.; Heywood, J. D.; Kenwright, A. M.; Khosravi, E. *J. Mol. Catal. A: Chem.* **2008**, *280*, 29−34.

(71) Rule, J. D.; Sottos, N. R.; White, S. R. *Polymer* **2007**, *48*, 3520−3529.
(72) Freeman, P. K.; Rao, V. N.; Rao, V. N. M.; George, D. E.; Fenwick, G. L. *J. Org. Chem.* **1967**, *32*, 3958−3963.
(73) Dolman, S. J.; Hultzsch, K. C.; Pezet, F.; Teng, X.; Hoveyda, A. H.; Schrock, R. R. *J. Am. Chem. Soc.* **2004**, *126*, 10945−10953.
(74) Ponticello, I. S. *J. Polym. Sci., Polym. Chem. Ed.* **1979**, *17*, 3509−3518.
(75) Fu, G. C.; Nguyen, S. T.; Grubbs, R. H. *J. Am. Chem. Soc.* **1993**, *115*, 9856−9857.
(76) Ulman, M.; Grubbs, R. H. *J. Org. Chem.* **1999**, *64*, 7202−7207.